PROMPT PHOTON PRODUCTION IN BREMSSTRAHLUNG FROM QUARK GLUON PLASMA AT $\sqrt{s}$ =10 *GeV* ENERGIES

M. R. ALIZADA

Department of Theoretical Physics, Baku State University

str. Z.Khalilov, 23, Az-1148 Baku, Azerbaijan

E-mail: mohsunalizade@gmail.com

I. INTRODUCTION

With energy ranging from 1.5 *GeV* to several 1 *GeV*, prompt photons from proton-proton collisions provide data on the development of the quark-gluon phase, the distribution of partons in nucleons, and the testing of perturbative QCD (pQCD). Prompt photons are produced by the hard scattering of partons in protons, as well as by Compton scattering of quark-gluon, annihialtion of quark-antiquark pair and bremsstrahlung of quarks [1-3]. At LHC energies, pQCD in leading order (LO) and next-to-leading order (NLO), which predominate, is used to characterize these processes.

Prompt photons only interact electromagnetically, their mean free path typically exceeds the transverse dimension of the region of hot matter produced by any nuclear collision by a significant amount. As a result, high-energy photons

produced in the inside of plasma typically through the surrounding material without interacting and carry information directly to the detector from their point of origin.

It is important to keep in mind that the majority of well-known charged particle accelerators, like the European LHC or the American "Tevatron" are made to operate at high energies (from 1 to 100 *TeV*). In addition to prompt photons, numerous elementary particles, including mesons, thermal photons, and others are produced as a result of colliding nucleons in high energies. It is difficult to precisely calculate the differential cross-section of production of prompt photon due to the production of extra elementary particles [4-6].

Our calculations were done with protons colliding at energies of $\sqrt{s}$=10 *GeV*, which doesn't take into account the production of extra elementary particles. Since

protons colliding at energies $\sqrt{s}$=10 *GeV* greatly restrict the possibility of producing extra elementary particles [7,8].

The differential cross-sections of process of bremsstrahlung, contributions, bremsstrahlung photon energy spectrum, and loss quark energy has been investigated at Tevatron energies [9-11].

The purpose of the report is to investigate role of the bremsstrahlung mechanism to production of prompt photons in energies 10 *GeV*. In order to achieve this, the dependence of differential cross-sections of the bremsstrahlung process has been calculated without and taking into account of polarization of colliding particles. Investigation of differential cross-section on the energy of colliding protons, transverse momentum p_T, cosine of the scattering angle, and rapidity of photon has carried out. Comparisons of differential cross-sections of

Compton quark-gluon scattering, annihilation of quark-antiquark pair and bremsstrahlung processes, and the effect of particle polarization on these processes has been carried out.

II. DIFFERENTIAL CROSS-SECTION OF $qq \to qq\gamma$ PROCESS

Collision of protons has been considered in parton model. Calculations were made in LO. The prompt photon production in the bremsstrahlung process has been considered with 16 Feynman diagrams. Matrix elements of all diagrams have written and the following invariants of Mandelstam of process has been determined:

$$s = (p_1 + p_2)^2 = (k_1 + p_3 + p_4)^2, \quad t = (p_1 - k_1)^2 = (p_4 + p_3 - p_2)^2, \; u = (p_2 - k_1)^2 = (p_4 + p_3 - p_1)^2,$$

$$q_1 = (p_1 - p_3)^2 = (k_1 + p_4 - p_2)^2, \quad q_2 = (p_2 - p_4)^2 = (k_1 + p_3 - p_1)^2,$$

$$s_1 = (p_4 + p_3)^2 = (p_1 + p_2 - k_1)^2, t_1 = (p_1 - p_4)^2 = (k_1 + p_1 - p_2)^2, \quad u_1 = (p_2 - p_2)^2 = (k_1 + p_4 - p_1)^2,$$

$$q_3 = (p_3 + k_1)^2 = (p_1 + p_2 - p_1)^2, \; q_4 = (p_4 + k_1)^2 = (p_1 + p_2 - p_3)^2$$

The square of matrix element of process M_1 at quark mass $m_q=0$ has been calculate in FeynCalc.

Differential cross-section of process has been calculated as in [12]:

$$\frac{d\sigma}{dt} = \frac{s_1}{16\pi^2 s^4} \left|\overline{M}\right|^2$$

The longitudinal polarization of colliding protons was taken into account as in [12]:

$$U(p_1)\overline{U}(p_1) = \frac{1}{2}(1 - \lambda_1\gamma_5)(\hat{p}_1 + m_1) \qquad U(p_2)\overline{U}(p_2) = \frac{1}{2}(1 - \lambda_2\gamma_5)(\hat{p}_2 + m_2)$$

Distribution functions of of *u*-, *d* quarks and *g* gluon on *x* are taken from [13]:

$$G_{u/h}(x)=A_u x^{\eta_1}(1-x)^{\eta_2}\left(1+\varepsilon_u\sqrt{x}+\gamma_u x\right),\ G_{d/h}(x)=A_d x^{\eta_3}(1-x)^{\eta_4}\left(1+\varepsilon_d\sqrt{x}+\gamma_d x\right),$$

$$G_{s/h}(x)=A_s x^{\delta_s}(1-x)^{\eta_s}\left(1+\varepsilon_s\sqrt{x}+\gamma_s x\right),\ G_{g/h}(x)=A_g x^{\delta_g}(1-x)^{\eta_g}\left(1+\varepsilon_g\sqrt{x}+\gamma_g x\right)+A_g^{'}x^{\delta_g^{'}}(1-x)^{\eta_g^{'}},$$

correspondingly. Values of parameters of distribution function is taken from [13]:

A_u=1.4335, η_{1u}=0.45232, η_{2u}=3.0409, ε_u=-2.3737, γ_u=8.9924,

A_d=5.0903, η_{1d}=0.71978, η_{2d}= 2.083, ε_d= -4.3654, γ_d= 7.4730,

A_g=0.0012216, δ_g=-0.83657, η_g=2.3882, ε_g= -38.997, γ_g=1445.5 .

Double spin asymmetry of process was calculated as in [14]:

$$A_{LL}=\frac{\sigma^{\uparrow\uparrow}-\sigma^{\uparrow\downarrow}}{\sigma^{\uparrow\uparrow}+\sigma^{\uparrow\downarrow}},$$

where $\sigma^{\uparrow\uparrow}$ and $\sigma^{\uparrow\downarrow}$ differential cross-sections of sub-processes calculated correspondingly at the same and opposite direction of polarization of colliding particles.

III. NUMERICAL CALCULTIONS AND DISSCUSION

1. Differential cross-section of bremsstrahlung process

The differential cross-section of the bremsstrahlung process increase with increasing the energy of colliding particles. At high energies of colliding particles in proton have high speed consequently, a sharp decreasing in speed due to braking will be significant. Also, it is well known that the bremsstrahlung that results is inversely proportional to the square of acceleration of particle. In the bremsstrahlung process, it is evident that high-energy particle collisions produce photons with a substantial transverse momentum. This corresponded to the saturation part of the curve of dependence of differential cross-section on the energy of the colliding particles.

The dependencies of the differential cross-sections calculated without and taking into account of polarization initial particles at the product of the helicity of the colliding particles $\lambda_1\lambda_2$=0.81 on transverse momentum are shown in fig.1.

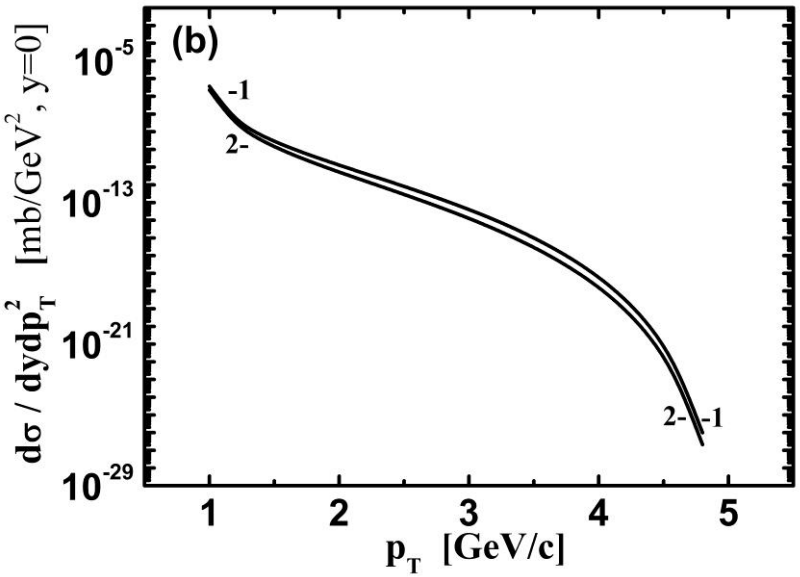

Fig.1 The dependencies of the differential cross-section calculated without (curve 1) and taking into account (curve 2) of longitudinal polarization colliding particles at $\lambda_1\lambda_2$=0.81 on transverse momentum.

As seen from fig.1 with increasing transverse momentum, the differential cross-section of process gets smaller. The production of photons with a small transverse momentum is more likely.

In the fig.2(a,b) are presented the dependence of difference and ratio of differential cross-sections calculated without and taking into account of longitudinal polarization on transverse momentum p_T.

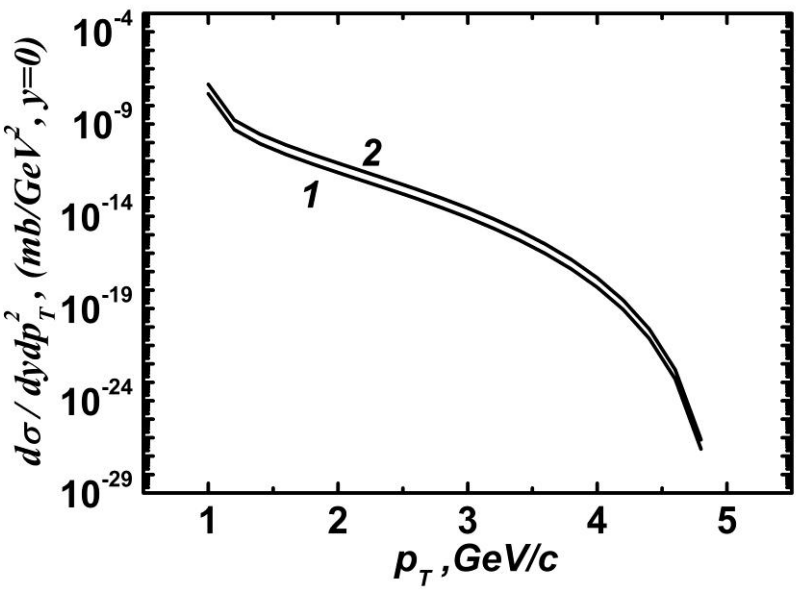

a

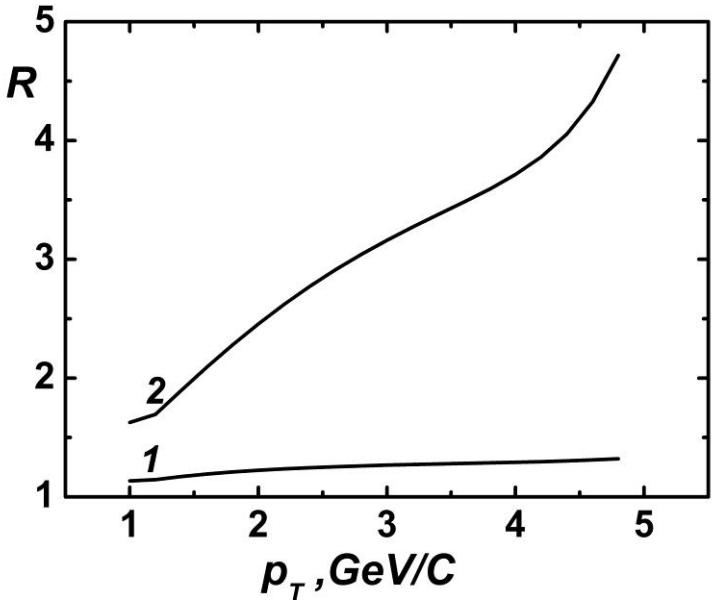

b

Fig.2(a,b) The dependence of difference (a) and ratio (b) of differential cross-sections calculated without and taking into account longitudinal polarization on transverse momentum p_T, curve 1 - $\lambda_1\lambda_2$=0.25, curve 2 - $\lambda_1\lambda_2$= 0.81

As seen from fig.2(a) the difference of differential cross-sections calculated without and taking into account longitudinal polarization decrease with increasing transverse momentum p_T. The difference of differential cross-sections calculated without and taking into account longitudinal polarization have big values at small values of p_T.

The ratio of differential cross-sections calculated without and taking into account longitudinal polarization increase with increasing transverse momentum p_T.

Additionally, it should be highlighted that, as can be shown from fig.2(a,b), the polarization order of colliding particles has small effect on the differential cross-section of the bremsstrahlung process.

In the fig.3 is presented the dependencies of accumulation of probability production of prompt photon on transverse momentum.

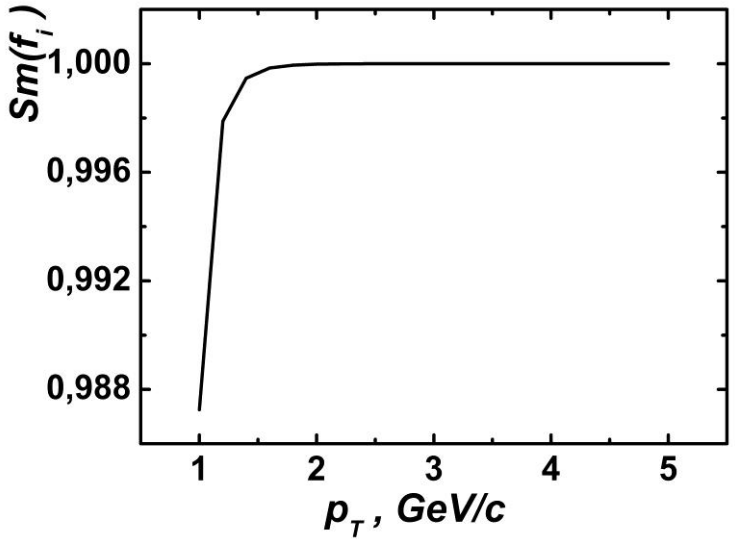

Fig.3 The dependence of accumulation of probability of production of prompt photons on transverse momentum at longitudinal polarization of colliding particles.

As seen from the fig.3 at longitudinal polarization number of produced prompt photons with transverse momentum $p_T \leq 0.6$ make up more 98.1% all produced prompt photons. This means that at longitudinal polarization of colliding particles distribution function of produced prompt photons on transverse momentum have more probability value at $p_T=0.6$ and gentle towards the side of large p_T. Investigation of accumulation of probability of production of prompt photons on transverse momentum at different value of longitudinal polarization showed, that polarization order has little effect on distribution function of prompt photons on transverse momentum.

Fig.4(a,b) show the dependencies of differential cross-sections calculated without and taking into account of polarization of colliding particles at $\lambda_1\lambda_2=0.81$ on the cosine of scattering angle and rapidity of photon.

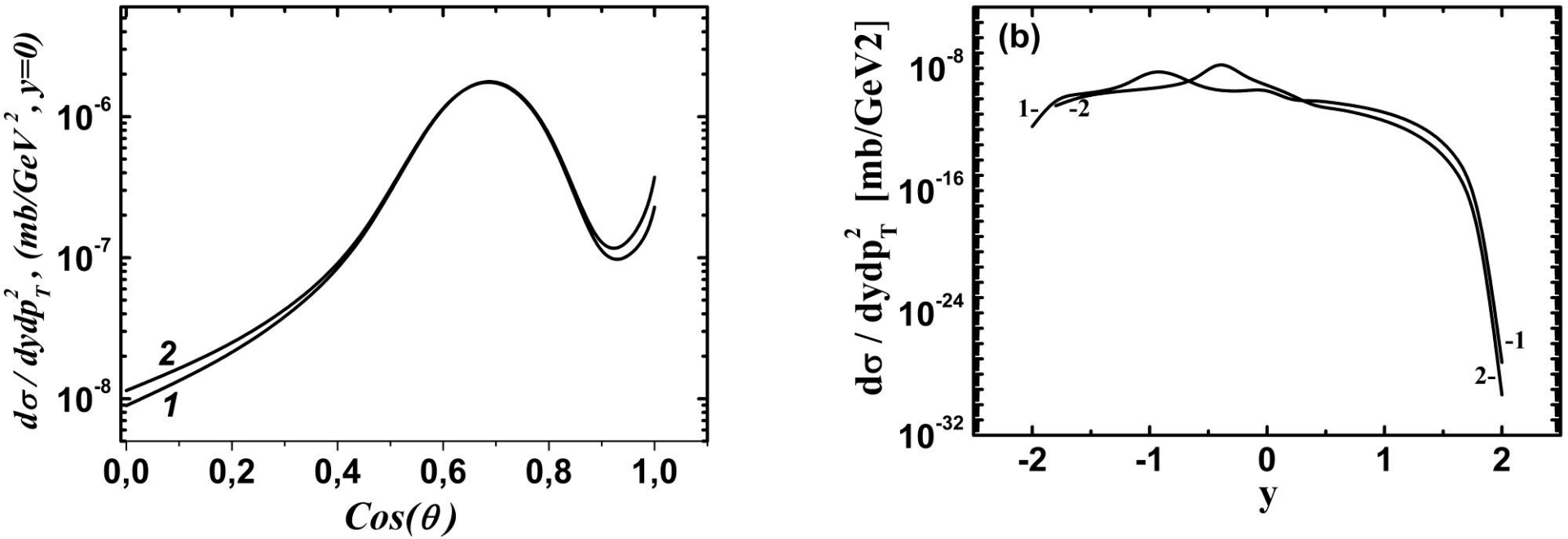

Fig.4(a,b) The dependencies of the differential cross-section calculated without (curve 1) and taking into account (curve 2) polarization at $\lambda_1\lambda_2$=0.81 on the cosine of scattering angle (a) and rapidity of photon *y* (b).

The cosine of scattering angle of photon increases as the differential cross-section of the process does, reaching its maximum at $cos(\theta)$=0.75 (θ=41.41^0) (fig. 4(a)). The future differential cross-section drops when the cosine of scattering angle of photon is increased and at $cos(\theta)$=0.9 (θ=25.84^0) have minimum. As can be seen, the differential cross-section has high values at big value of photon scattering angles. Most of the produced photons are detected in the $0.45 \leq cos(\theta) \leq 0.85$ ($31.79^0 \leq \theta \leq 63.26^0$). Fig.5 schematically shows the dependence of the intensity (I) of the bremsstrahlung on the scattering angle (θ). The bremsstrahlung is present within the cone with span angle 32^0.

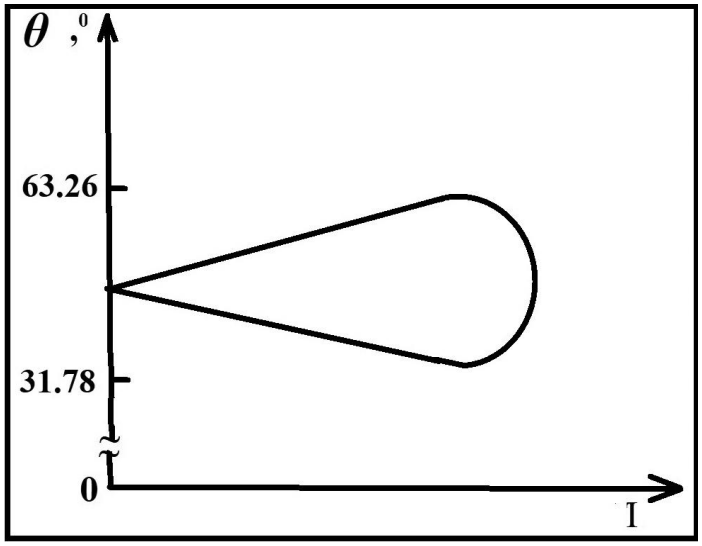

Fig.5 Schematic representation of the dependence of the intensity (I) of the bremsstrahlung on the scattering angle of photon (θ).

This is because photons are more likely to be produced when they move in a direction close to the collision axis. When photons fly out in a direction perpendicular to the collision axis, their probability of production is significantly lower.

In the fig.6 is presented the dependencies of accumulation of probability production of prompt photon on cosine of scattering angle of photon.

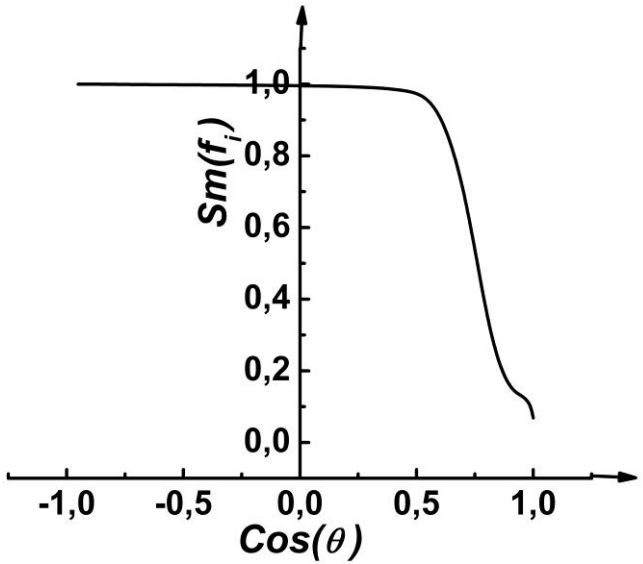

Fig.6 The dependence of accumulation of probability of production of prompt photons on cosine of scattering angle of photon at longitudinal polarization of colliding particles.

As seen from the figure at longitudinal polarization number of produced prompt photons with cosine of scattering angle of photon $Cos(\theta)$ ≤0.707 make up more 71.9% all produced prompt photons. This means that at longitudinal polarization of colliding particles distribution function of produced prompt photons on cosine of scattering angle of photon have more probability value at $Cos(\theta)$=0.707 and gentle towards the side of large p_T.

The dependence of the differential cross-section on the rapidity of produced of prompt photons shows that the probability of production of photons with greater rapidity increases with increasing rapidity (fig.4(b)). This is because the energy of photons is proportional to their rapidity, and faster photons have more energy.

The differential cross-section has a maximum value at photon rapidity equal to 0. This is because photons with this rapidity have the greatest energy.

In the large interval changing of rapidity of photon y value of the differential cross-section is constant and begins to significantly decline at y=1.6 (fig.4(b)). The dependence of differential cross-section on rapidity of photon y has a maximum in y=-0.25. Polarization of colliding particles, shift this maximum towards small y. Rapidity of photon has been calculated using the formula $y=-ln(tg(\theta/2))$ and at y=0.973 the value of scattering angle was $\theta=arccos(0.75)$. This corresponds to the previously described dependence of the differential section on the cosine of the scattering angle of photon.

The dependence of differential cross-section without and taking into account of polarization at $\lambda_1\lambda_2$=0.81 on x_T is shown in fig.7.

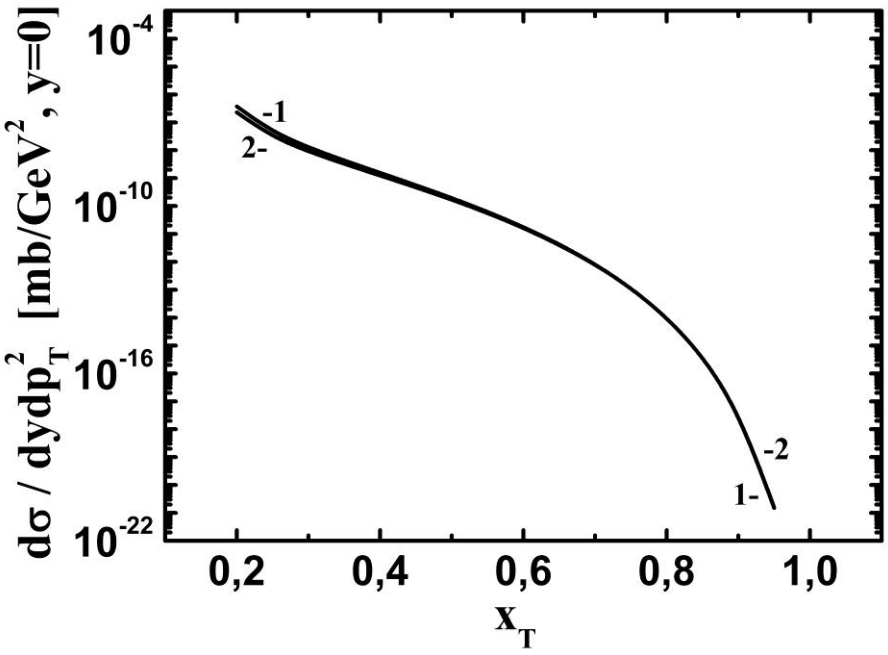

Fig.7 The dependencies of the differential cross-sections calculated without (curve 1) and taking into account (curve 2) polarization of colliding protons at $\lambda_1\lambda_2$=0.81 on x_T.

2. Double spin asymmetry of bremsstrahlung process

The dependencies the double spin asymmetry on energy colliding particles and the transverse momentum p_T are presented in fig.7(a,b).

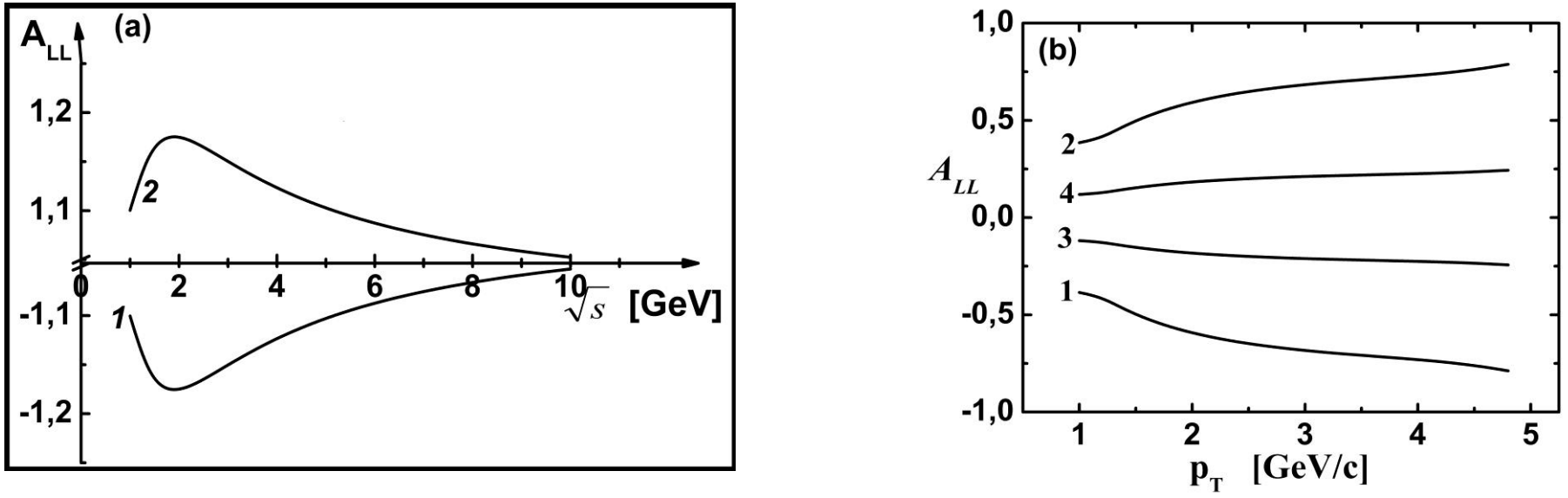

Fig.7(a,b) The dependencies of double spin asymmetry on the energy of colliding particles $\lambda_1\lambda_2$=0.81 (curve 1), $\lambda_1\lambda_2$=-0.81 (curve 2) (a) and transverse momentum p_T (b) at $\lambda_1\lambda_2$=0.81, $\lambda_1\lambda_2$=-0.81, $\lambda_1\lambda_2$=0.25, $\lambda_1\lambda_2$=-0.25, correspondingly curves 1,2,3,4.

As can be seen in fig.7(a), double spin asymmetry A_{LL} increases with particle energy, reach a minimum at $\lambda_1\lambda_2$=0.81 and a maximum at $\lambda_1\lambda_2$=-0.81 at $\sqrt{s}$=2 *GeV*. The differential cross-section calculated taking into account polarization is large at $\lambda_1\lambda_2$=-0.81 and is small at $\lambda_1\lambda_2$=0.81 than the differential cross-section calculated without taking into account polarization of colliding particles. Further, with an increase in the energy of colliding protons, the double spin asymmetry of A_{LL} decreases and eventually approaches zero.

With increasing transverse momentum p_T, the double spin asymmetry A_{LL} increases at $\lambda_1\lambda_2<0$ and decreases at $\lambda_1\lambda_2>0$ reached plateau at a certain p_T (fig.5(b)). The value of this p_T increases with increasing the absolute value of $\lambda_1\lambda_2$.

The dependence of A_{LL} on $cos(\theta)$ has been investigated at various values of $\lambda_1\lambda_2$. Investigations shows that double spin asymmetry don not depend the cosine of the scattering angle of photon. Double spin asymmetry has the same values at different values of the cosine of scattering angle of prompt photon and is equal to A_{LL} at values of $\lambda_1\lambda_2$. The relationship between double spin asymmetry and the product of $\lambda_1\lambda_2$ helicity at different value of p_T are presented in fig.6.

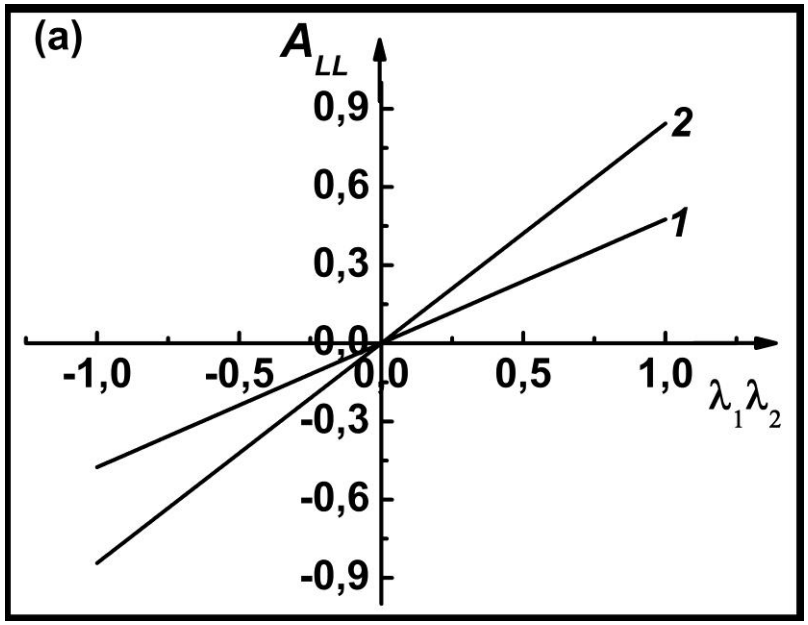

Fig.6 The dependence of double spin asymmetry A_{LL} on the product of $\lambda_1\lambda_2$ helicity at p_T = 1 *GeV/c* (curve 1), p_T = 3 *GeV/c* (curve 2) at $\sqrt{s}$ =10*GeV* and y = 0.

The dependence of double spin asymmetry on x_T is shown in fig.7.

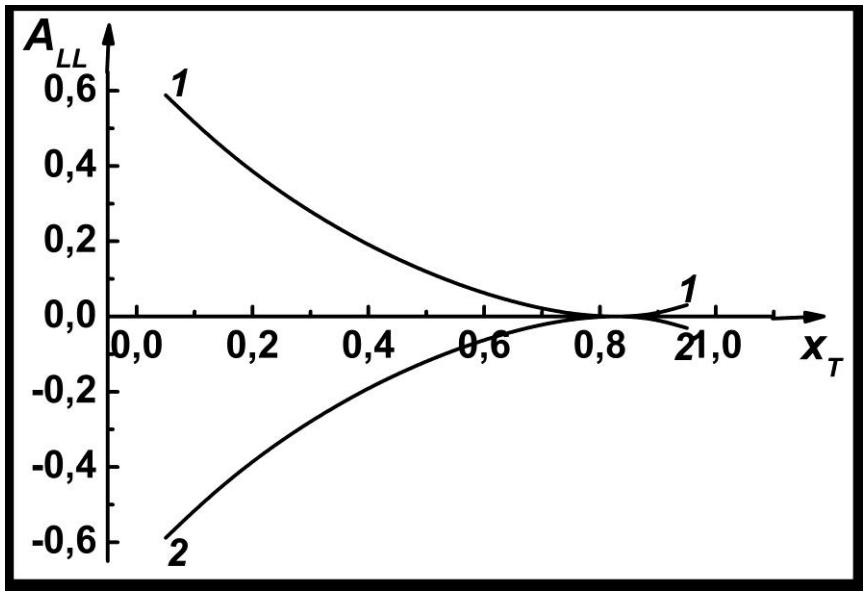

Fig.7 The dependence of double spin asymmetry on x_T, at $\lambda_1\lambda_2$=0.81 (curve 1), at $\lambda_1\lambda_2$=-0.81 (curve 2).

With increasing value of x_T, double spin asymmetry decreases at $\lambda_1\lambda_2$=0.81 and increases at $\lambda_1\lambda_2$=-0.81.

3. Comparison of the differential cross-sections of Compton scattering of quark-gluon, the annihilation of quark-antiquark pair and bremsstrahlung processes

Fig.9 shows the dependence of differential cross-section of prompt photon production in proton-proton collisions at Compton scattering of quark-gluon, the annihilation of quark-antiquark pair and bremsstrahlung on transverse momentum p_T and the dependence of the ratio of a differential cross-section of Compton scattering, annihilation of quark-antiquark pair and bremsstrahlung to the total differential cross-section on transverse momentum.

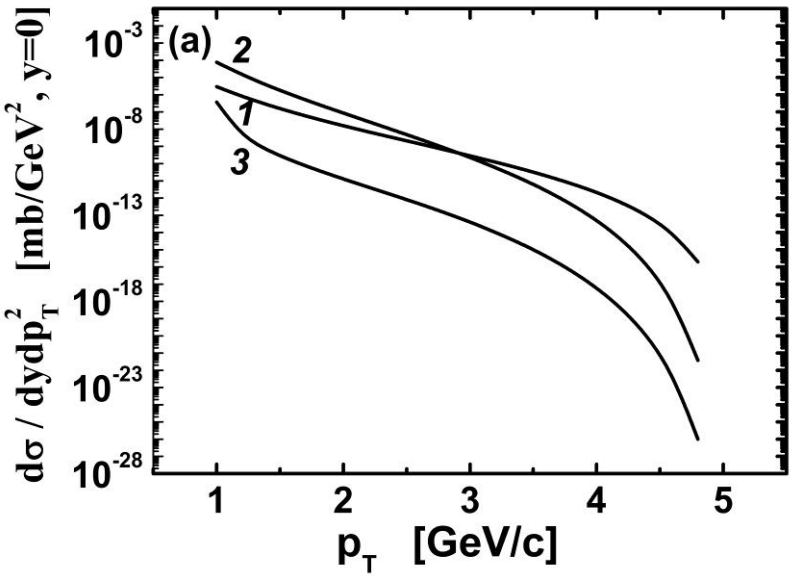

Fig.9 The dependence of differential cross-section of prompt photon production in proton-proton collisions at Compton scattering (curve 1), the annihilation of quark-antiquark pair (curve 2) and bremsstrahlung (curve 3) on transverse momentum p_T

As can be shown in fig.9, the dependence of differential cross-section of Compton scattering is higher than differential cross-sections other processes. The

contribution of Compton scattering to the total differential cross-section is significant (>50%). Annihilation of quark-antiquark pair and bremsstrahlung processes, correspondingly, contribute 47% and 0.03% of the total differential cross-sections production of prompt photons.

The comparison also showed, that in bremsstrahlung at low collision energies of protons, the production of photons with a large transverse momentum is more likely and at high energies, the collision of photons with a small transverse momentum is more likely. However, in the Compton scattering quark-gluon at low energies, the collision of protons the formation of photons with a small p_T is more likely and at large energies of the collision of protons production of photons with a large p_T is less likely.

4. Energetic spectrum of prompt photon produced in bremsstrahlung process

For bremsstrahlung process, the 4-dimensional equivalent of the law of conservation of energy will be:

$$p_1^0 + p_2^0 - \sqrt{\overrightarrow{k_1^2}} - \sqrt{\left(\overrightarrow{p_2} + \overrightarrow{p_1} - \overrightarrow{k_1}\right)^2 + m_{k_2}^2} = 0$$

where p_1, p_2, k_1 4-dimensional momentum of colliding particles, photon, correspondingly, m_{k2} mass of final quark.

The last equation has been squared twice and has been obtained a quadratic equation with coefficients a, b and c that describes the momentum of the produced prompt photons.

$$a = 4\left|\overrightarrow{p_1}\right|^2 c^2 - 4\left(p_2^0 + p_1^0\right)^2, \qquad b = 8\left|\overrightarrow{p_1}\right| c m_p^2, \qquad \text{and} \quad c = 4m_p^2$$

In the quadratic equation has been used the following designations:

$$p_1^0 = E_1^2 = \overrightarrow{p_1}^2 + m_p^2, \qquad p_2^0 = E_2^1 = \overrightarrow{p_2}^2 + m_p^2 = m_p^2, \qquad \left|\overrightarrow{p_1}\right|^2 = E_1^2 - m_p^2$$

The quadratic equation has the following solutions:

$$x_{1,2} = \frac{-cm_p^2\sqrt{E_1^2 - m_p^2} \pm \sqrt{E_1^4 m_p^4 + 2E_1^2 m_p^6 + m_p^8}}{c^2E_1^2 - E_1^4 - c^2m_p^2 - 2E_1^2m_p^2 - m_p^4}$$

Consider those solutions of the equation that are not complex, i.e. the discriminant of the equation is greater than zero and equal to zero. In this case, the solution x_2 satisfies theses conditions.

According to the energy spectrum of the photon produced in Compton scattering of quark-gluon, annihilation of quark-antiquark pair and bremsstrahlung, the temperature of QGP is $1.739 \cdot 10^{12}$ *K* (150 *MeV*) and $9.203 \cdot 10^{10}$ *K* (10 *MeV*), correspondingly. May be make conlusion, that prompt photon

producton in bremsstrahlung occurs at the end of QGP life and the wavelength of prompt photon in Compton scattering quark-gluon, annihilation of quark-antiquark pair and bremsstrahlung is different.

CONCLUSIONS

The differential cross-section of the bremsstrahlung process increases with increasing energy of colliding protons. This is because partons have a high speed at high energies of colliding protons and therefore a sharp decrease in speed due to braking will be significant.

The differential cross-section of the process decreases with increasing the transverse momentum of photons.

At longitudinal polarization of colliding particles distribution function of produced prompt photons on transverse momentum have more probability value at p_T=0.6 and gentle towards the side of large p_T. Polarization order has little effect on distribution function of prompt photons on transverse momentum.

At longitudinal polarization of colliding particles distribution function of produced prompt photons on cosine of scattering angle of photon have more probability value at $Cos(\theta)$=0.707 and gentle towards the side of large $Cos(\theta)$.

The bremsstrahlung is present within the cone with span angle 32^0.

The contribution of bremsstrahlung to the total differential cross-section of the process of production of the prompt photon is 0.03% of the total differential cross-section.

Polarization of the colliding particle little affects the bremsstrahlung process and strong affects the annihilation of quark-antiquark pair process.

Double spin asymmetry A_{LL} decreases at $\lambda_1\lambda_2<0$ and increases at $\lambda_1\lambda_2>0$ with increasing value of transverse momentum p_T and reaches the plateau.

The temperature of QGP determined on the base of the energetic spectrum of the produced photon in bremsstrahlung is $9.203 \cdot 10^{10}$ K that it is lower temperature

determined from energetic spectrum of Compton scattering of quark-gluon and annihilation of quark-antiqaurk pair. This allowed make conclusion, that in probability, prompt photon production in bremsstrahlung occurs at the end of the lifetime of QGP.

LITERATURE

1. P.Aurenche, R.Baier, M.Fontannaz, *Phys.Rev.* **D 42,** 1440 (1990). DOI:https://doi.org/10.1103.
2. T.Becher, C.Lorentzen, M.D.Schwartz, *Phys.Rev.* **D 86**, 054026 (2012). https://doi.org/10.1103/PhysRevD.86.054026, arXiv:1206.6115 [hep-ph]. https://doi.org/10.48550/arXiv.1206.6115.
3. M.Germain, on behalf of the ALICE Collaboration, *Nucl.Phys.* **A 967,** 696 (2017). http://dx.doi.org/10.1016/j.nuclphysa.2017.05.094.
4. A.Peter, arXiv:0808.2767v2 [hep-ph] 5 Mar 2009. https://doi.org/10.48550/arXiv.0808.2767.
5. B.Z.Kopeliovich, A. Schaefer, A. V. Tarasov *Phys.Rev.* **C59,** 1609 (1999). https://doi.org/10.1103/Phys.Rev. C.59.1609, arXiv:hep-ph/9808378v5 17 Dec 1998 https://doi.org/10.48550/arXiv.hep-ph/9808378.
6. B.Fiol, E.Gerchkovitz, Z.Komargodski, arXiv:1510.01332v2[[hep-th] 2 Nov 2015. https://doi.org/10.1103.PhysRevLett. 116.081601.
7. M.R.Alizada, A.I.Ahmadov, A.B.Arbuzov Study of polarization effects in prompt photon production // Transaction of Azerbaijan National Academy of Sciences. Physics and Astronomy. **2**, 9 (2022).

8. M.R.Alizada, A.I.Ahmadov, A.B.Arbuzōv Prompt photons production in proton-proton collision at high energies // Proceedings of the 7th International conference MTP-2021, Modern Trends in Physics, Baku State University, Baku, Azerbaijan December 15-17, 2021, V. 1, P. 142-145, http://mtp2021.bsu.edu.az/Proc-MTP-2021_Volume_1.pdf
9. R.Baier, Y.L.Dokshitzer, A.H.Mueller, D.Schiff *Nucl.Phys.* **B 531**, 403 (1998). [arXiv:hep-ph/9804212] https://doi.org/10.1016/S0550-3213(00)00457-0.
10. R.Baier, Y.L.Dokshitzer, A.H.Mueller D.Schiff, *Phys.Rev.* **C 58**, 1706 (1998). [arXiv:hep-ph/9803473]. https://doi.org/10.1103/PhysRevC.58.1706 https://doi.org/10.48550/arXiv.hep-ph/9803473.
11. C. Jean-Francois, R.A.Zhitnitsky, arXiv:0907.4715v1 [astro-ph.HE] 27 Jul 2009. https://doi.org/10.1103/PhysRevD.80.123006, https://doi.org/10.48550/arXiv.0907.4715.
12. A.D.Martina, W.J.Stirlingb, R.S.Thornec, G.Wattc Parton distributions for the LHC // Eur. Phys. J.C63,189 (2009) //arXiv:0901.0002v3 [hep-ph]
13. O.Martina Transverse double-spin asymmetries for dimuon production in pp collisions arXiv:hep-ph/9905544v2 25 Oct 1999

14. Y.Kanazawa, Koike Yuji, N.Nishiyama ALT in the polarized Drell-Yan process at RHIC and HERA energies arXiv:hep-ph/9801341v2 15 Mar 1998
15. E.Byckling, K.Kajantie *Particle Kinematics.* John Wiley and Sons, London, New York, Sydney, Toronto, 1973.
16. L.E.Gordon, W.Vogelsang. Polarized and unpolarized isolated prompt photon production beyond the leading order // *Phys.Rev.* **50,** 1901 (1994).
17. P.Hinderer, M.Schlegel, W. Vogelsang. Double-longitudinal spin asymmetry in single-inclusive lepton scattering at NLO // arXiv:1703.10872v1 [hep-ph]. 2017.
18. M.R.Alizada, A.I.Ahmadov Radiation correction to Compton scattering of quark-gluon and annihilation of quark-antiquartk pair processes of prompt photon production in proton-proton collisions at high energies // Известия Национальной Академии Наук Азербайджана, серия физика-технических и математических наук, физика и астрономия, 2023, N 2, C. 52-58

THANK YOU FOR

YOUR ATTENTION

FEYNMAN DIAGRAMS OF PROMPT PHOTON PRODUCTION IN BREMSSTRAHLUNG FROM QUARK GLUON PLASMA

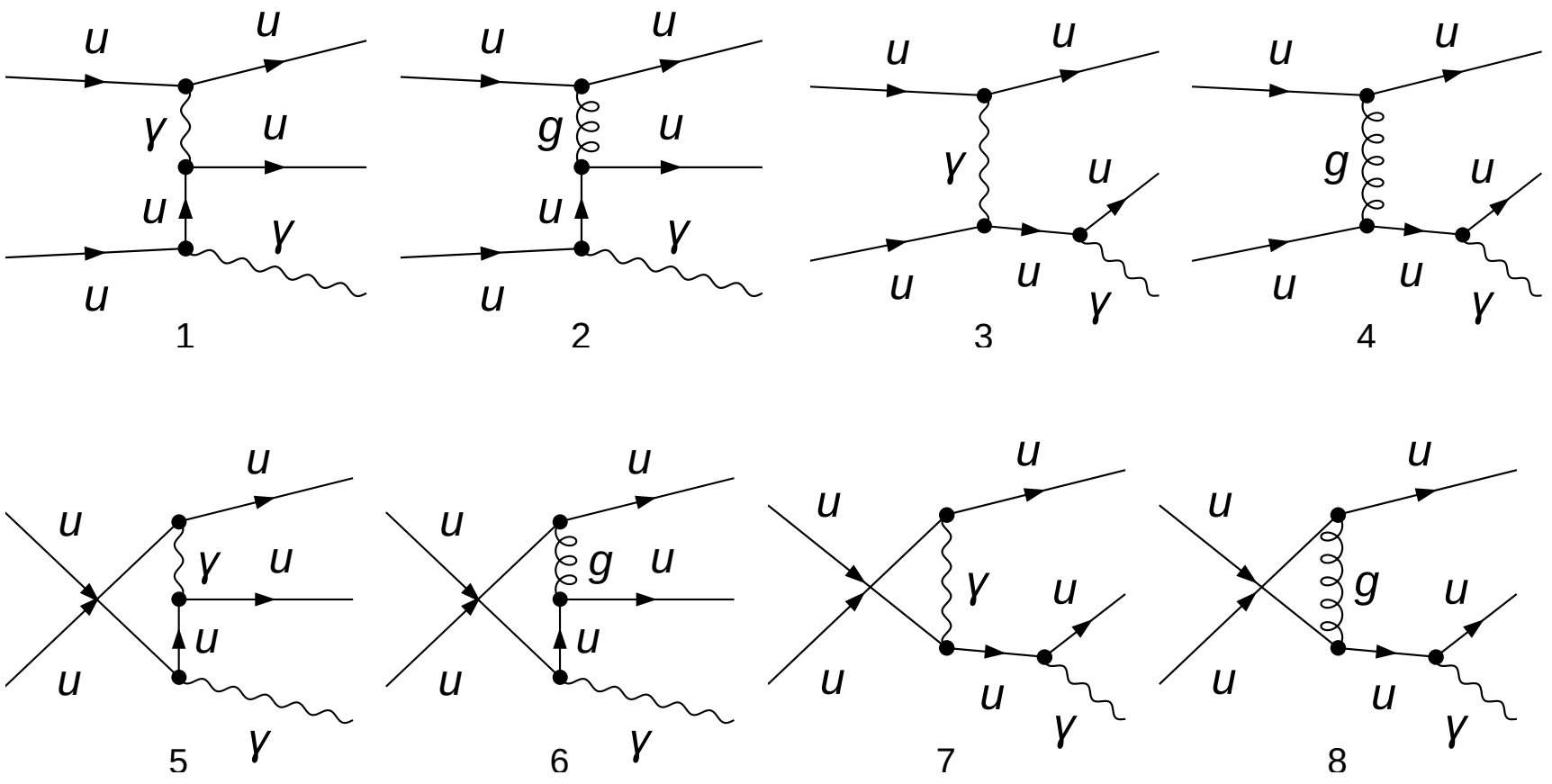

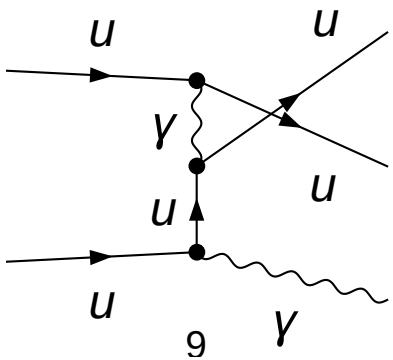

9

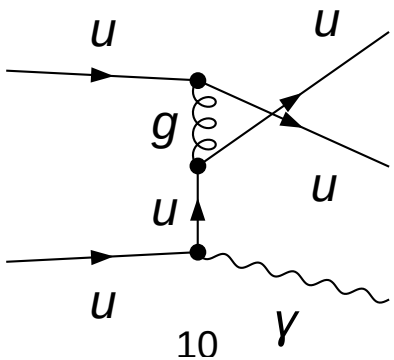

10

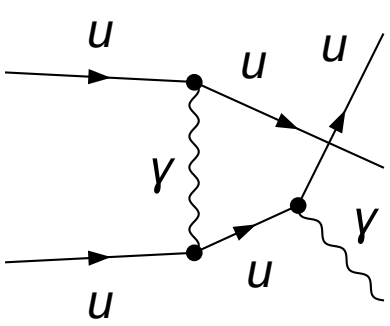

11

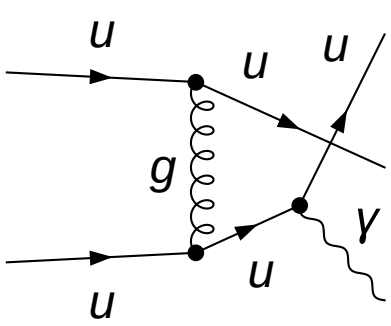

12

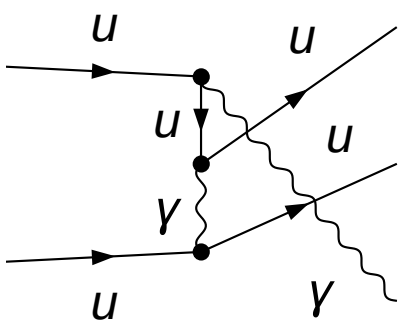

13

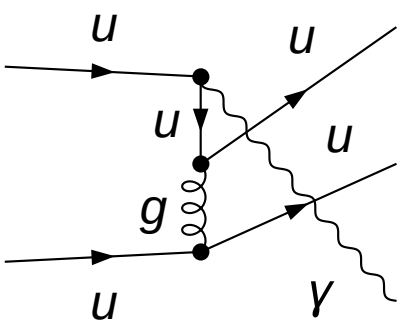

14

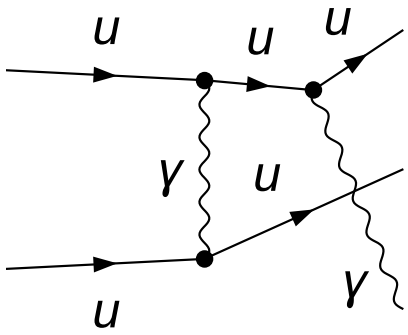

15

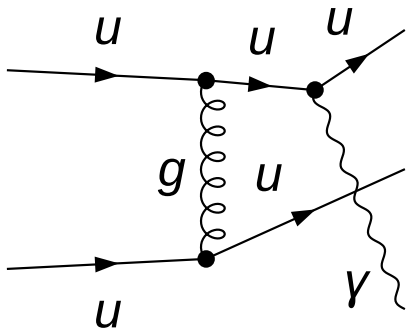

16

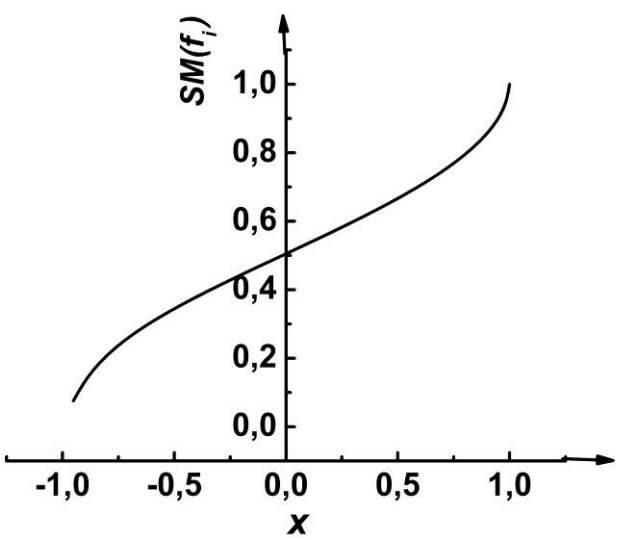

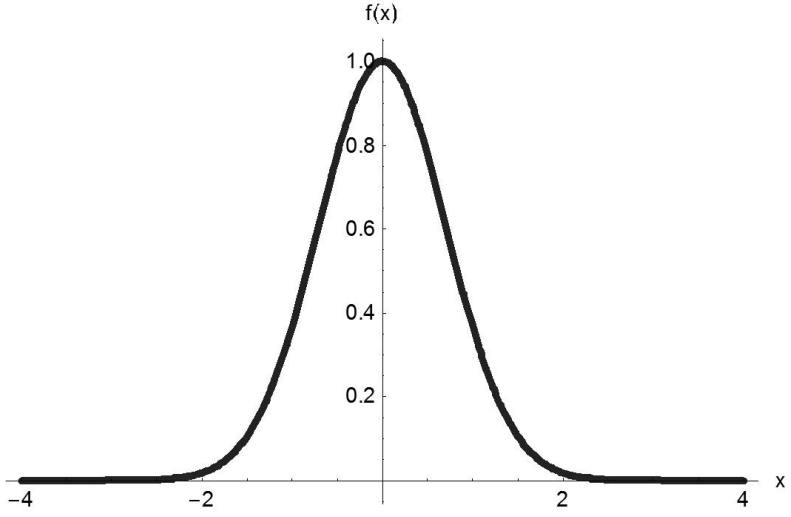

S form

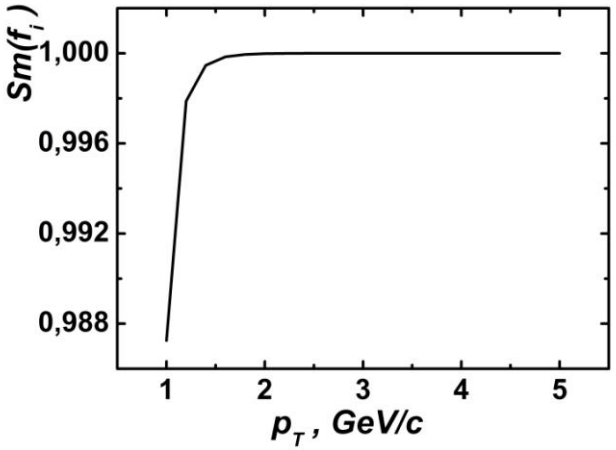
Sm(f_i)
1,000
0,996
0,992
0,988
1
2
3
4
5
p_T , GeV/c

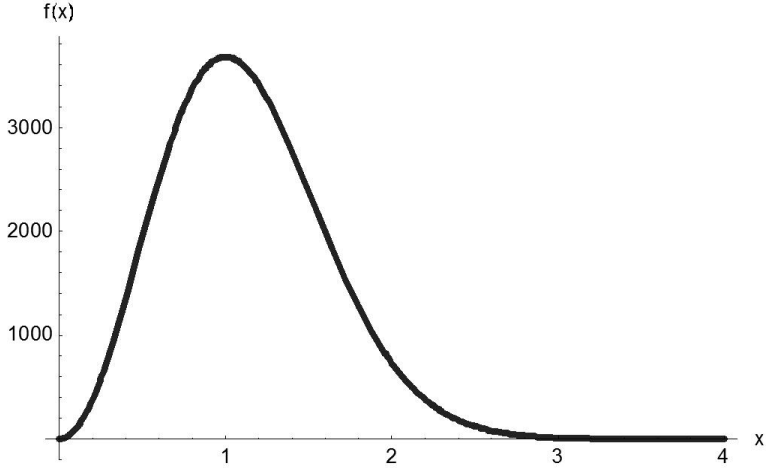
f(x)
3000
2000
1000
1
2
3
4
x

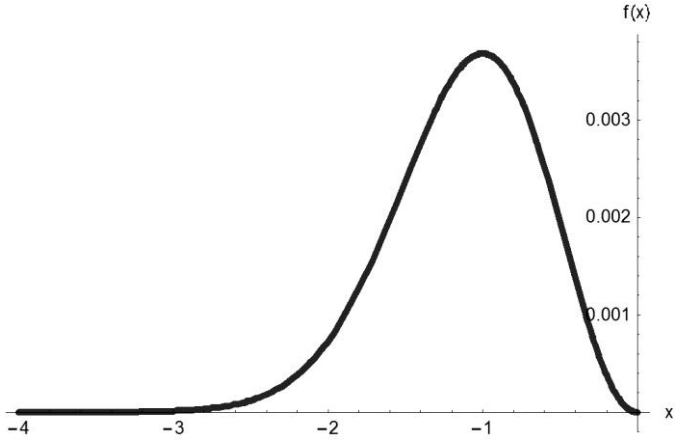
f(x)
0.003
0.002
0.001
−4
−3
−2
−1
x

Parton distribution function was evaluated at patameters value indicated in the above. In the fig.1 showed the distribution functions of *u*-, *d* quarks and *g* gluon by fraction *x* of the carried proton momentum.

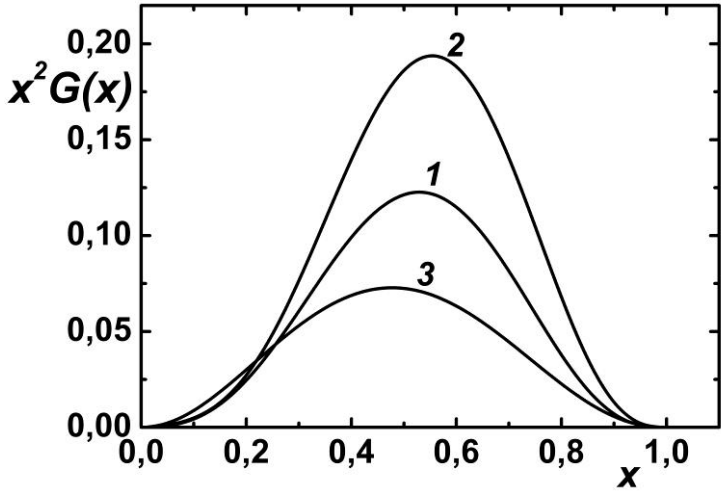

Fig.1 Distribuntion function of *u*-, *d* quarks and *g* gluon by fraction *x* of the carried proton momentum, curves 1, 2 and 3, correspondingly.

Parameters mean value ($\bar{x}$), mean quadratic deviation (σ) and coefficient of asymmetry (η) of parton diftribution function in dimensionless quantity are calculated as in [11] and are prsented in the table.

Table. Parameters of parton diftribution function mean value ($\bar{x}$), mean quadratic deviation (σ) and coefficient of asymmetry (η).

partons	$\bar{x}$	σ	η
u	0.52	0.165	-0.072
d	0.539	0.161	-0.135
g	0.485	0.181	0.041

As seen from fig.1 parton distribution function of *u* and *d* quark has a gentle shape towards the side of small *x (η<0)* and parton distribution function of *g* gluon has a gentle shape towards the side of big *x (η>0)*. Using the transition from dimensionless quantities to dimensional quantities, we get: $(\overline{p_T}, \sigma_{p_T})$=(2.598, 0.824); (2.696, 0.807); (0.2423, 0.908), correspondingly for *u*-, *d* quarks and *g* gluon. Based on the parameters of the parton distribution function, the parameters of the photon distribution function on the transverese momentum are determined: $2.423 \leq \overline{p_T} \leq 2.598$ *GeV/c,* $0.807 \leq \sigma(p_T) \leq 0.907$ *GeV/c*, $-0.0716 \leq \varepsilon \leq 0.0413$.